Journal of Inflammation Research

Dovepress
Taylor & Francis Group

Open Access Full Text Article

ORIGINAL RESEARCH

Therapeutic Effects of Fire Needling Acupuncture on Pain Relief and Cartilage Protection in MIA-Induced Knee Osteoarthritis Rats: The Role of Macrophage Polarization in Synovium and Angiogenesis in Subchondral Bone

Jiangyan Wei[1,*], Xin Yang[1,*], Xiaobo Ge[2,*], Luopeng Zhao[3], Xueyan Liu[1,2], Jiarun Zhang[1], Jun Zhou[1], Chengcheng Zhang[1], Wenshan Li[1,2], Zhijuan Li[1], Tianli Lyu[1], Yizhan Wang[1], Fang Yuan[1], Lu Liu[1], Bin Li[1]

[1]Department of Acupuncture and Moxibustion, Beijing Hospital of Traditional Chinese Medicine, Capital Medical University, Beijing Key Laboratory of Acupuncture Neuromodulation, Beijing, 100010, People's Republic of China; [2]Graduate School, Beijing University of Chinese Medicine, Beijing, 100029, People's Republic of China; [3]Beijing Institute of Traditional Chinese Medicine, Beijing, 100010, People's Republic of China

*These authors contributed equally to this work

Correspondence: Bin Li; Lu Liu, Department of Acupuncture and Moxibustion, Beijing Hospital of Traditional Chinese Medicine, Capital Medical University, Beijing Key Laboratory of Acupuncture Neuromodulation, 23 Meishuguan Back Street, Dongcheng District, Beijing, 100010, People's Republic of China, Email libin@bjzhongyi.com; lululalavictor1985@126.com

Purpose: Knee osteoarthritis (KOA) is a prevalent degenerative disease impacting bone and joint health. Clinical studies indicate that fire needling acupuncture can alleviate joint stiffness, pain, and dysfunction in KOA. Previous research demonstrated its efficacy in reducing pain, mitigating cartilage damage, and regulating macrophage polarization, but its effects on subchondral bone remain unclear. This study aimed to evaluate the therapeutic effects of fire needling acupuncture on subchondral bone in KOA.

Methods: Sprague-Dawley rats were divided into three groups: control (CON), monosodium iodoacetate (MIA), and fire needling acupuncture (FNA) (n=6 per group). A KOA model was established using 0.3 mg/50 μL MIA, followed by acupuncture at acupoints SP10, ST34, ST35, EX-LE5, and ST36 twice weekly. Evaluations included body weight, joint diameter, weight distribution, and mechanical withdrawal threshold. Micro-CT imaging assessed tibial plateau bone mass changes. Histological evaluations used HE, Safranin O/Fast Green, and toluidine blue staining. Immunohistochemistry examined COL2, MMP9, and MMP13 expression, while macrophage polarization was analyzed using immunofluorescence for F4/80, iNOS, and Arg-1. TRAP staining assessed osteoclast activity, and immunofluorescence for CD31/Emcn and VEGF evaluated angiogenesis in subchondral bone.

Results: Fire needling acupuncture significantly improved weight distribution and mechanical withdrawal thresholds, reduced synovial inflammation and abnormal changes in subchondral bone, and preserved cartilage integrity in MIA-induced KOA rats. Notably, F4/80 and iNOS expression levels decreased, while Arg-1 expression increased after treatment. Additionally, TRAP, CD31/Emcn, and VEGF expression in subchondral bone decreased following fire needling acupuncture.

Conclusion: Fire needling acupuncture mitigates pain behavior, synovial inflammation, cartilage degradation, and abnormal changes in subchondral bone in MIA-induced KOA rats. The therapeutic mechanism may involve modulation of synovial macrophage polarization and subchondral bone angiogenesis. Further research is warranted to elucidate the precise molecular pathways and the interaction between macrophage polarization and angiogenesis.

Keywords: fire needling acupuncture, knee osteoarthritis, cartilage degradation, macrophages polarization, subchondral bone angiogenesis

Received: 12 February 2025
Accepted: 28 May 2025
Published: 9 June 2025

Introduction

Osteoarthritis (OA) is a degenerative cartilage disease that is prevalent among older adults and represents a significant public health challenge.[1] According to the Global Burden of Disease (GBD) 2021, OA affected 7.6% of the global population in 2020, which equates to approximately 595 million individuals.[2] Each year, over 250 million people worldwide suffer from OA, with around 41% experiencing physical disabilities.[3] From 1990 to 2019, the burden of OA has doubled, particularly in middle Socio-Demographic Index (SDI) countries such as China.[2] After the age of 70, OA ranks as the seventh leading cause of disability globally, predominantly affecting the knee.[2] Due to population growth and aging, age-standardized years lived with disability (YLDs) related to knee OA (KOA) are projected to increase.[4] This underscores the urgent need for preventive measures and highlights the critical importance of research and intervention strategies targeting this condition.

Traditional treatment for mild-to-moderate KOA primarily involves pharmacotherapy. This mainly includes non-steroidal anti-inflammatory drugs (NSAIDs), which can alleviate pain and inflammation but may lead to side effects and drug resistance with prolonged use.[5,6] Additionally, drugs commonly used for intra-articular injections, such as corticosteroids, may have potential chondrotoxic effects, necessitating further evaluation of their efficacy and safety.[7] Therefore, exploring the role of non-pharmacological therapies in KOA management is particularly important. Compared to drug treatments, non-pharmacological methods generally have fewer side effects and are suitable for long-term management.[8] Through physical therapy, lifestyle modifications, and psychological support, patients can effectively relieve symptoms and improve their quality of life. Thus, non-pharmacological therapies should receive greater emphasis and application in comprehensive KOA treatment plans.

Fire needling acupuncture therapy, a traditional Chinese medical treatment, has garnered increasing research attention in recent years for the management of KOA. This therapy involves the direct insertion of heated needles into the affected area, aiming to improve local blood circulation, alleviate pain, and promote tissue repair.[9,10] Numerous studies have demonstrated that fire needling acupuncture therapy effectively reduces pain and functional impairment in patients with KOA.[11,12] Additionally, the treatment course is relatively short, often requiring only a few sessions to achieve noticeable results, providing patients with a more convenient therapeutic option. While the precise mechanisms of fire needling acupuncture therapy are not yet fully understood, its effectiveness in reducing inflammation and slowing cartilage deterioration has been well established.[13,14]

It is well established that changes in synovium and subchondral bone play a crucial role in the progression of KOA and are closely associated with pain and functional impairment.[15–17] Consequently, treatment strategies targeting synovium and subchondral bone have become central in KOA research. Some studies indicate that synovitis and subchondral bone remodeling interacts with the degeneration of articular cartilage.[16,18,19] Increasingly, research has focused on regulating the polarization of synovial macrophages to mitigate cartilage damage in KOA.[20] Although the mechanisms by which subchondral bone influences KOA require further exploration, evidence indicates that maintaining subchondral bone health not only alleviates KOA symptoms but may also slow disease progression.[16,21] Therefore, this study focuses on the effects of fire needling acupuncture therapy on macrophage polarization in synovium and angiogenesis in subchondral bone, as well as its relationship with cartilage degeneration, aiming to provide new insights and strategies for the comprehensive treatment of KOA.

Materials and Methods

Animals

A total of eighteen male Sprague-Dawley rats, each weighing between 180 and 200 grams, were procured from Beijing Huafukang Biotechnology Co., LTD (Beijing, CHINA). During the entire experimental duration, the rats were provided with standard feed and water ad libitum, while being maintained under regulated environmental conditions, including a temperature of 23 ± 1 °C, a humidity level ranging from 40% to 60%, and a 12-hour light-dark cycle. Prior to the commencement of the experiments, the rats were acclimatized for a minimum of one week. To eliminate potential experimenter bias, the individuals conducting the experiments were blinded. Following the adaptation period, the rats were randomly assigned to three groups, each comprising six rats. The experimental protocols received approval from the

Ethics Committee for Animal Experimentation at the Beijing Institute of Traditional Chinese Medicine (approval no. BJTCM-R-2023-12-02) and were executed in accordance with the committee's established norms and regulations.

KOA Rat Model Establishment

Eighteen male Sprague-Dawley rats were randomly divided into three groups (n=6 each) before monosodium iodoacetate (MIA, Sigma, USA) injection: control group (CON), MIA group (MIA), fire needling acupuncture group (FNA). The KOA was induced via a single intra-articular administration of MIA in the left knee (0.3 mg in 50 μL). Rats were anesthetized by inhalation of isoflurane (3–4% induced, 1–1.5% maintained) (RWD, China) and their left knee joints were shaved before intra-articular injection. At day 0, the 0.3mg MIA in 50μL of 0.9% sterile normal saline was injected into the left knee joint through the subpatellar ligament using a microinjector with 26 G needle inserted with the knee flexed at an angle of 90°.[22] The knees were stretched and flexed gently to disperse the MIA throughout the articular cavity after injection. The control group received 50μL sterile normal saline at a similar injection site.

Fire Needling Acupuncture Treatment

The rats of the FNA group received fire needling acupuncture treatment on the left five acupoints of SP10 (Xuehai), ST34 (Liangqiu), ST35 (Dubi), EX-LE5 (Xiyan), and ST36 (Zusanli). The identification of these acupoints was conducted in alignment with the Animal Acupuncture Point Atlas and the T/CAAM 0002–2020 document, which is entitled "Name and Location of Commonly Used Acupoints in Experimental Animals – Part 2: Rat".[23] The electronic intelligent fire needling acupuncture (2mm length, 0.4mm diameter, approximately 200°C, utility model, patent no. ZL201721678201.2) was applied in this study and supplied by Beijing Hanbotai Kanglai Technology Development Co., LTD. The needle was heated before being punctured and withdrawn from the acupoints (a needle ejection and withdrawal in 0.1s). The depth and temperature of the fire needling acupuncture used during the fire needling acupuncture treatment were consistent. The rats were anesthetized (isoflurane, 3–4% induction, 1–1.5% maintenance) before commencing fire needling acupuncture. The rats had their left knee bent and had them punctured once at each acupoint. This was done twice a week from the seventh day after MIA injection (Figure 1A), for a total of 3 weeks. The operation of the CON group and the MIA group was the same as that of the FNA group, without fire needling acupuncture treatment.

Body Weight Assessment

Body weight was measured using an electronic scale before MIA injection and at days 4, 8, 11, 15, 18, 22, 25, and 29 after injection (Figure 1A and B).

Knee Swelling Assessment

Knee joint diameters were measured to infer joint swelling as an indicator of inflammation resulting from injection of MIA or saline. The diameter of the left knee was measured with a manual caliper (SYNTEK, China). In the process of measuring the diameter of all joints, keep the joint in the same position, and take the average value of three consecutive measurements. The timing for the knee swelling assessment coincides with the body weight assessment (Figure 1A and C).

Weight Bearing Test

Weight distribution asymmetry across the right and left knee was assessed using an Incapacity Meter® (IITC Life Science Inc., USA) to evaluate the distribution of weight bearing in the hind limbs. The force exerted by each hind limb was measured in grams and reported as a percentage of total body weight. Rats were allowed to acclimate to the test apparatus, which involved positioning them on an incline that required the hind paws to rest on separate platforms. Once stationary, the device recorded the average pressure exerted by both feet over a 10-second interval following the activation of the start button. Changes in weight distribution were calculated using the formula: [(weight bearing of left hind paw/weight bearing of left and right hind paws) × 100].[24] The final value represented the average of three repeated measurements. Assessments were conducted prior to the injection of MIA, on days 4 and 7 post-injection, and the day following the fire needling acupuncture treatment (Figure 1A and D).

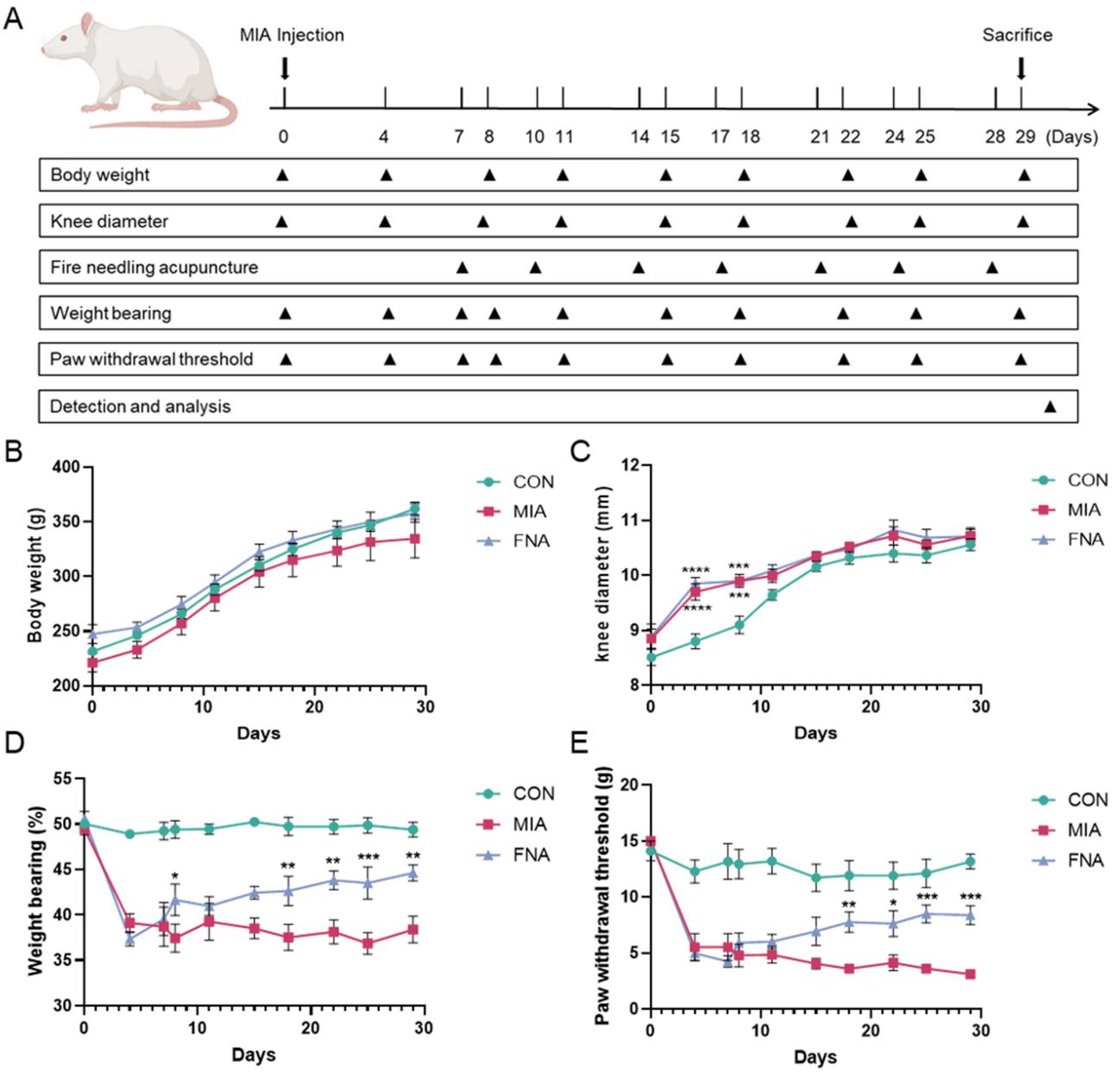

Figure 1 (**A**) Flowchart of animal experiment. (**B**) Body weight analysis. (**C**) Joint diameter analysis. ***P<0.001, ****P<0.0001, vs CON group. (**D**) Weight bearing analysis. *P<0.05, **P<0.01, ***P<0.001, vs MIA group. (**E**) Paw withdrawal threshold analysis. *P<0.05, **P<0.01, ***P<0.001, vs MIA group. Data are expressed as the mean ± SEM, n = 6 for each group.

Paw Withdrawal Threshold Test

The Von Frey filaments (Stoelting, USA) were utilized to quantitatively assess the severity of joint pain by measuring the hind paw withdrawal threshold in rats. Each rat was placed individually in an organic plastic chamber with a metal mesh floor, and the experiment commenced after the animals had acclimated to their environment. A Von Frey hair filament was applied perpendicular to the plantar surface of the left hind limb until the filament began to bend, maintaining this pressure for 5 seconds. A positive withdrawal response was defined as the rat quickly withdrawing or licking its hind limb. Filaments were applied in ascending order, starting from 2 g, until a withdrawal response was observed. Following the identification of the first positive response, a descending series of tests was conducted until no response was elicited. A sequence of four tests was performed after the initial positive response, and the paw withdrawal threshold was calculated accordingly.[25] Assessments were conducted on the same day as weight bearing tests, with a minimum interval of half an hour between the two procedures (Figure 1A and E).

Sample Collection

On day 29 after MIA injection, all rats were anesthetized with pentobarbital sodium and sacrificed to collect the left knee joints. Positioned supine, the rats underwent transcardial perfusion with 500 mL of 0.9% sterile saline until the lungs, liver, and limbs turned white, followed by 300 mL of 4% paraformaldehyde (PFA), during which tail and limb tremors were noted. The left knee joints were then harvested. After macroscopic observation, it was fixed in 4% PFA for 48 hours. After that, samples were decalcified in 10% EDTA for three weeks, embedded in paraffin, and sectioned to approximately 4 μm for further evaluation.

Micro-Computed Tomography (Micro-CT) Scanning and Analysis

The rat joints were scanned using a high-resolution micro-computed tomography (micro-CT) system (Skyscan 1276, Bruker, Germany) at a source voltage of 50 kV and 497μA, achieving a resolution of 50μm per pixel. Reconstructed images obtained from Skyscan NRecon software version 1.6.9 (Bruker, Germany) were analyzed using CTAn software version 1.15.4.0 (Skyscan) to visualize and assess bone histomorphometric parameters. The scanning encompassed the entire knee joint, while the analysis specifically focused on the subchondral bone of the tibial plateau. Three-dimensional (3D) reconstruction of the knee joint structures was performed and analyzed. The region of interest (ROI) was segmented following manual verification of the contours for each slice. To quantify bone parameters, the ROI was delineated along the margin of the tibial plateau, and the following metrics were analyzed: bone volume (BV), bone volume fraction (BV/TV), trabecular number (Tb.N), trabecular pattern factor (Tb.Pf), trabecular thickness (Tb.Th), trabecular separation (Tb.Sp), and bone mineral density (BMD).

Histological Analysis

The samples were subsequently embedded in paraffin wax and sectioned to a thickness of approximately 4μm for pathological evaluation. The sections were stained using Hematoxylin and Eosin (HE), Safranin O/Fast Green (Saf-O), and toluidine blue to assess knee joint inflammation and cartilage damage. Histological examination was conducted under an optical microscope. The investigators independently evaluated the sections while remaining blinded to their nature.

Hematoxylin and Eosin (HE) Staining

Synovial inflammation and cartilage damage were histologically assessed using hematoxylin and eosin staining (GP1031, Servicebio, China) according to standardized protocols. Briefly, dewaxed and hydrated tissue sections were sequentially stained with hematoxylin (3–5 min), differentiated (2–5 s), blued (2–5 s), and counterstained with eosin (5 min) before neutral gum mounting. Pathological evaluation was performed microscopically, with synovitis severity quantified using established synovitis scoring criteria as previously reported.[26]

Safranin O/Fast Green (Saf-O) Staining

Cartilage extracellular matrix integrity was evaluated using Safranin O/Fast Green staining (G1053, Servicebio, China). Tissue sections underwent sequential treatment with ethylene glycol ethyl ether acetate solutions (6 h at 37°C followed by overnight incubation, then two 10–15 min room temperature steps), followed by graded alcohol rehydration (100% to 80%, 10 min/step). Sections were counterstained with Fast Green (3–4 min) and Safranin O (15–30 s), then dehydrated through three anhydrous ethanol changes (5 min each) and xylene clearing. Histopathological scoring (0–6 scale) quantified cartilage degeneration based on lesion depth, with grade 6 representing full-thickness cartilage loss with bone deformation.[27]

Toluidine Blue Staining

Chondrocyte extracellular matrix integrity was evaluated through toluidine blue staining (G1032, Servicebio, China) using standardized protocols. Tissue sections underwent sequential dehydration with Environmental Friendly Dewaxing Liquid I and II (20 min each), followed by hydration through graded ethanol solutions. After tap water rinsing, sections were stained with TB (2–5 min) and differentiated with 0.1% glacial acetic acid under microscopic monitoring. The reaction was terminated by water washing, and dried sections were cleared in xylene (10 min) before neutral gum mounting for microscopic evaluation of matrix integrity.

Tartrate-Resistant Acid Phosphatase (TRAP) Staining

Subchondral osteoclast activity in MIA-induced KOA was evaluated using tartrate-resistant acid phosphatase staining (G1050, Servicebio, China) per manufacturer's protocol. Tissue sections were pretreated with hydrophobic barrier creation and 37°C hydration (2 h), followed by TRAP solution incubation (37°C, 20 min). Post-wash nuclei were counterstained with hematoxylin (15 s) with acid differentiation/ammonia blueing steps. After routine ethanol dehydration and xylene clearing, sections were neutral gum-mounted for microscopic quantification of osteoclast activity using established histomorphometric criteria.

Immunohistochemical (IHC) Staining

Immunohistochemical staining was performed to assess the expression of collagen Type II (COL2) (GB11021, Servicebio, China), MMP9 (GB11132, Servicebio, China), and MMP13 (GB11247, Servicebio, China). Following deparaffinization and dehydration, sections were incubated at 37°C for 30 minutes, then rinsed with phosphate-buffered saline (PBS). Endogenous peroxidase activity was blocked by treating the sections with 3% hydrogen peroxide for 10 minutes at room temperature. After another PBS wash, sections were incubated with 5% bovine serum albumin (BSA) for 30 minutes at 37°C. Primary antibodies against COL2, MMP9, and MMP13 were applied overnight at 4°C. After washing with PBS, sections were incubated with a horseradish peroxidase-conjugated secondary antibody for 1 hour at room temperature. Samples were then stained with DAB for coloration and counterstained with hematoxylin. The number of positively stained cells in the articular cartilage of the femur and tibial plateau regions was counted, and the proportion of positive cells was analyzed using Image-Pro Plus software and Image J.

Immunofluorescence (IF) Staining

The procedure for preparing tissue sections was performed according to previously established methods. Knee sections embedded in paraffin were subjected to deparaffinization and rehydration processes. Subsequently, pepsin was applied to ensure complete coverage of the slices, which were then incubated at 37°C for a duration of 30 minutes. After washing, sections were treated with 0.3% Triton X-100 (A1009, Applygen, China) to permeabilize the membranes, followed by blocking with 10% normal goat serum at 37°C for 30 minutes. Specific primary antibodies targeting F4/80 (70076, CST, USA), iNOS (ab15323, Abcam, UK), Arg-1 (93668, CST, USA), VEGF (sc-7269, Santa Cruz, USA), CD31 (ab182981, Abcam, UK), and endomucin (Emcn) (sc-65495, Santa Cruz, USA) were applied and incubated overnight at 4°C. On the following day, sections were rinsed three times with phosphate-buffered saline (PBS) for 5 minutes each, then incubated with secondary antibodies at 37°C for 1 hour. Counterstaining with DAPI was performed for 10 minutes in the dark. After applying an anti-fluorescence quenching tablet, coverslips were sealed. Fluorescence images were captured using a fluorescence scanner (Leica Microsystems Co., Ltd., Germany), and quantitative analysis of fluorescence intensity was conducted using Image J.

Statistical Analysis

Statistical analyses were performed using GraphPad Prism 9.0 software. All data are presented as means ± standard error of the mean (SEM). The differences between groups of pain behaviors were analyzed with Two-way measurements ANOVA, other statistical analysis was performed using one-way ANOVA and Tukey's post-hoc test. Statistical significance was defined as a P-value less than 0.05, denoted as $*P < 0.05$, $**P < 0.01$, $***P < 0.001$ and $****P < 0.0001$.

Results

Effects of Fire Needling Acupuncture on Articular Cartilage Degradation in KOA Rats

To evaluate the therapeutic efficacy of fire needling acupuncture in rats, macroscopic observations of the knee joints were conducted at the conclusion of the treatment (Figure 2A). Notable joint thickening was observed in the MIA group compared to the CON group. The knee joint surfaces in the CON group appeared smooth and intact on both the femur and tibia. In contrast, the MIA group exhibited significant bone erosion, fissures, and cartilage degeneration on the knee joint surfaces. The treatment group demonstrated improvements in the degree of inflammation, cartilage degeneration, and erosion compared to the MIA group, and showed less loss and erosion of the cartilage in the medial tibial plateau and femur areas, suggesting that fire needling acupuncture has a therapeutic effect on KOA in rats.

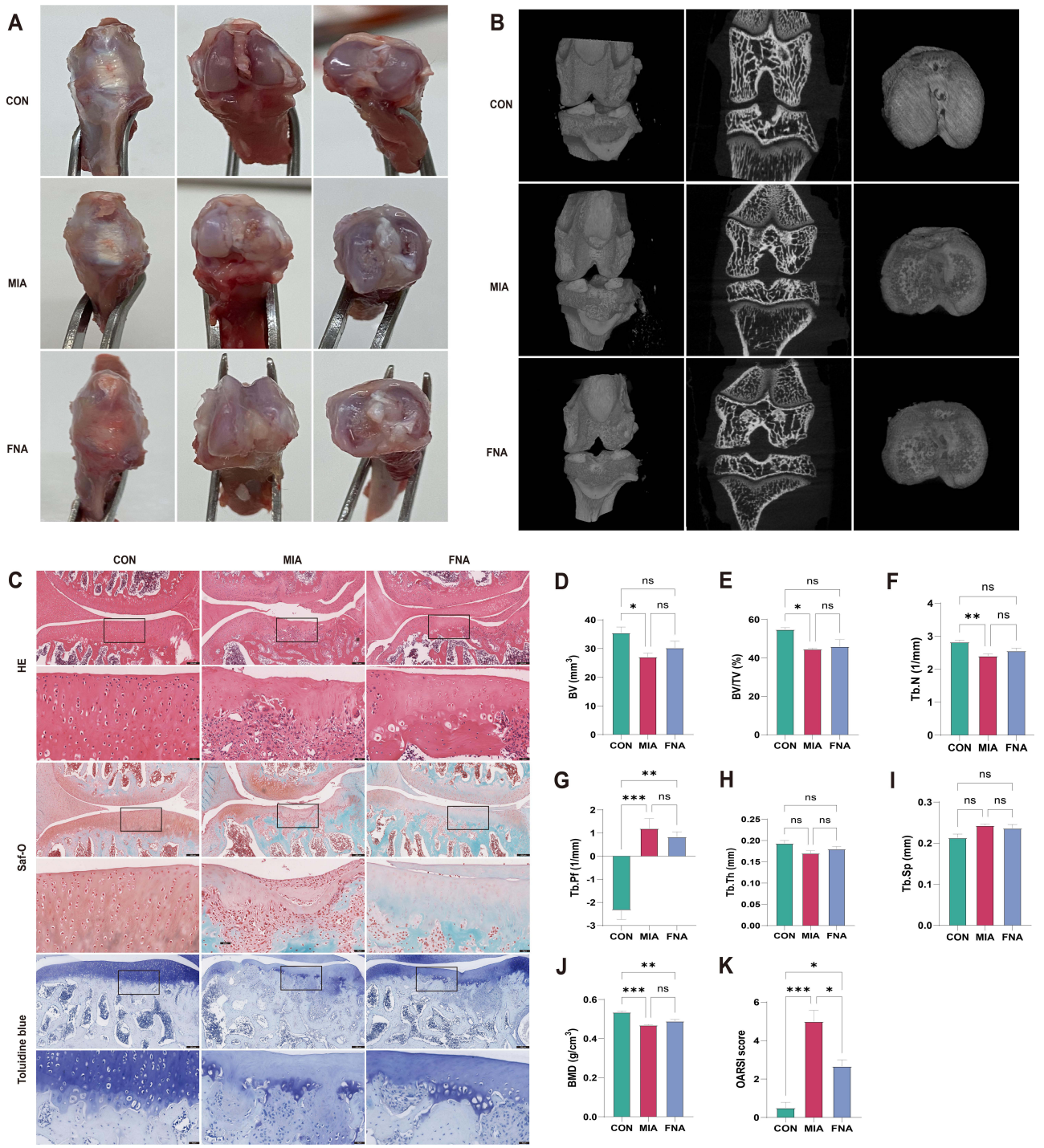

Figure 2 (**A**) Macroscopic observation of knee joints. (**B**) Micro-CT comparison of the knee joint in MIA-induced KOA rats. (**C**) Hematoxylin and eosin (HE) staining, Safranin O/Fast Green (Saf-O) staining, and Toluidine blue staining of the knee joint cartilage of the rats. Scale bars = 200μm or 40μm. (**D–J**) Micro-CT analysis of bone volume (BV), bone volume fraction (BV/TV), trabecular number (Tb.N), trabecular pattern factor (Tb.Pf), trabecular thickness (Tb.Th), trabecular separation (Tb.Sp), and bone mineral density (BMD) of the tibial plateau of KOA rats. (**K**) Quantification of OARSI scores. Data are expressed as the mean ± SEM, n = 3 for each group. **P*<0.05, ***P*<0.01, ****P*<0.001.

Abbreviation: ns, no significance.

Micro-CT analysis revealed that the CON group had smooth and regular articular surfaces, with mineralized structures present in the intra-articular space of the knee, and no signs of inflammatory alterations or open fissures (Figure 2B). In comparison, the MIA group displayed narrowing of the intra-articular spaces, subchondral bone sclerosis,

https://doi.org/10.2147/JIR.S518829

areas of cartilage erosion, and partial loss of normal structural appearance. Marked reductions in bone mass, along with damage and thinning of the trabecular structure and increased spacing, were evident following MIA injection. Specifically, the MIA group exhibited significant reductions in tibial plateau bone volume (BV), bone volume fraction (BV/TV), trabecular number (Tb.N), trabecular thickness (Tb.Th), and bone mineral density (BMD), while trabecular pattern factor (Tb.Pf) and trabecular separation (Tb.Sp) were increased (Figure 2D–J). Additionally, a statistically significant difference in BV, BV/TV, Tb.N, Tb.Pf, and BMD was observed between the MIA group and the CON group (Figure 2D–G and J). The results of micro-CT analysis indicated that while there were observable trends toward improved bone trabecular structure, BMD, and BV/TV following fire needling acupuncture treatment compared to the untreated OA group (Figure 2B), these changes did not reach statistical significance. The FNA group exhibited a reduction in bone loss and an apparent enhancement in trabecular density, although these observations require further statistical validation.

Histological changes in the cartilage surface of knee joints were assessed using HE, Saf-O, and toluidine blue staining under a microscope (Figure 2C). Observations revealed that the cartilage surface in the CON group was smooth, with normal chondrocytes exhibiting distinct nuclei and neatly arranged structures. The extracellular matrix was uniformly stained, featuring a thick cartilage layer, and the tide line was clearly visible. In contrast, the MIA group displayed severe degeneration of bone tissue, characterized by chondrocyte death and matrix loss, indicating significant joint damage. Additionally, Saf-O and toluidine blue staining appeared faint in this group. The FNA group exhibited less degeneration compared to the MIA group, with cartilage layer thickness approaching that of the CON group. However, there was a loss of the marking line, an irregular surface, and viable chondrocytes with nuclei of varying sizes. Histological scoring (Figure 2K) revealed that the OARSI scores in the MIA group were significantly higher than those in the CON group, while the OARSI scores in the FNA group were lower than those in the MIA group. These findings further indicate that fire needling acupuncture effectively inhibits cartilage degeneration, thereby mitigating the progression of KOA.

Impact of Fire Needling Acupuncture on the Expression of Cartilage Damage Biomarkers in KOA Rats

To further investigate the protective effects of fire needling acupuncture on cartilage, immunohistochemical staining for collagen type II (COL2), matrix metalloproteinase 9 (MMP9), and matrix metalloproteinase 13 (MMP13) was conducted on knee cartilage. As shown in Figure 3A, the CON group exhibited substantial brown staining in the cartilage, indicative of COL2 expression, while the MIA group displayed minimal brown staining. The FNA group showed intermediate staining levels. The CON group had less brown staining for MMP9 and MMP13, whereas the MIA group demonstrated a significant increase in brown staining, indicating elevated expression of these matrix metalloproteinases. In contrast, the FNA group exhibited relatively lower expression levels of MMP9 and MMP13. Immunohistochemical analysis confirmed that fire needling acupuncture effectively reduced MMP9 and MMP13 levels in the cartilage of KOA rats, while enhancing COL2 levels (Figure 3B–D). These findings indicate that fire needling acupuncture positively influences the microenvironment of KOA, thereby promoting cartilage health and contributing to the therapeutic objectives of KOA treatment.

Attenuation of Persistent Pain in KOA Rats Following Fire Needling Acupuncture Treatment

After intra-articular injection of MIA, the joints of the rats exhibited swelling, and some of the left limbs displayed signs of lameness. Rats that touched their left joints exhibited evasive behaviors. However, there was no significant difference in body weight among the groups (Figure 1B). Signs of inflammation were evident following MIA injection, with a notable increase in knee diameter observed at day 7 compared to the CON group, although no differences were detected at subsequent time points (Figure 1C).

Weight distribution and mechanical withdrawal threshold tests were conducted to assess pain responses in the rats. Initially, all groups supported themselves symmetrically on both hind limbs, indicating an absence of joint discomfort.

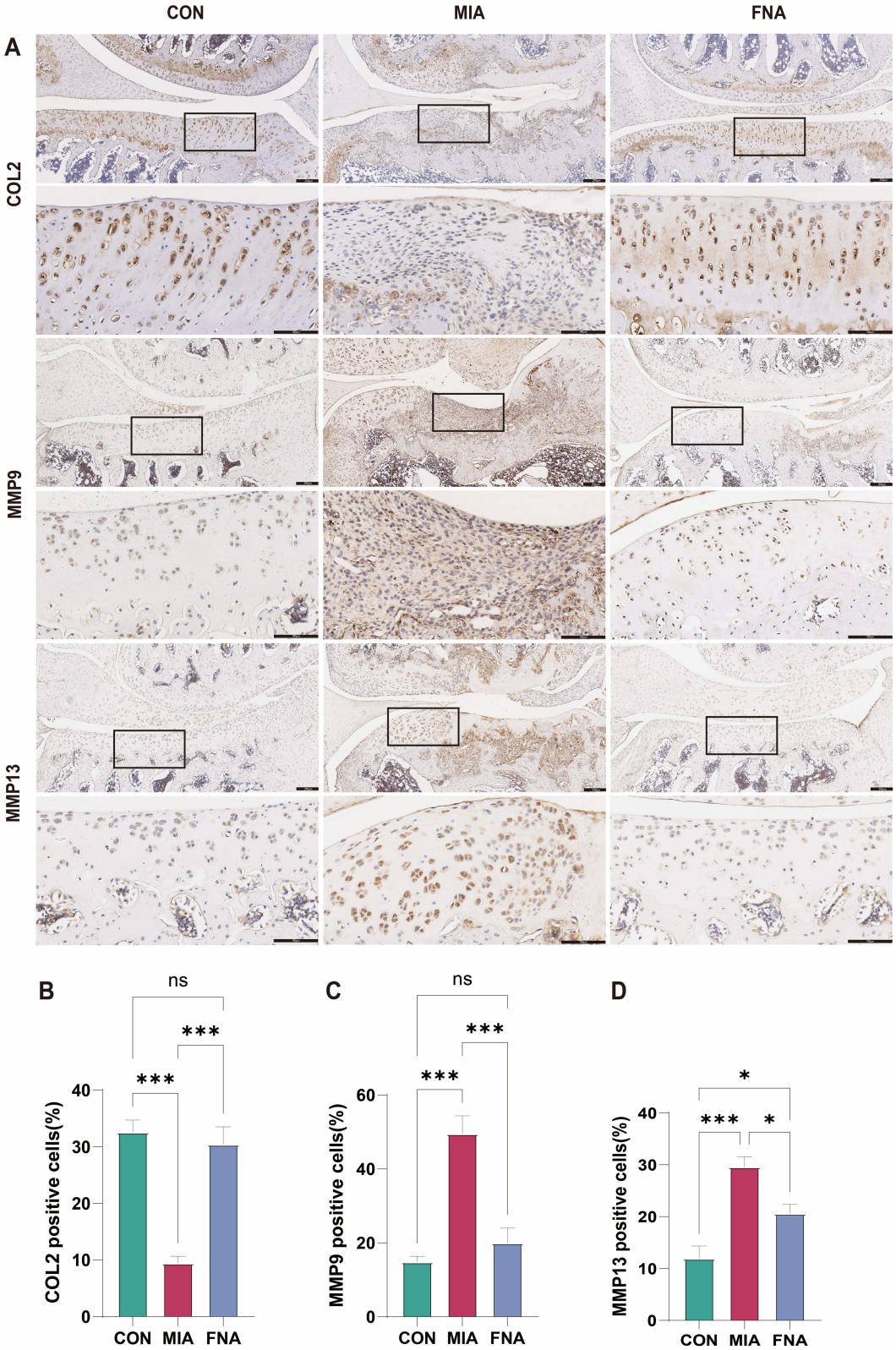

Figure 3 (**A**) Images of Immunohistochemistry staining of COL2, MMP9 and MMP13 of rat knee joints. Scale bars = 200μm or 100μm. (**B–D**) Quantification of IHC staining of the number of positive cells of COL2, MMP9 and MMP13. Data are expressed as the mean ± SEM, n = 3 for each group. **P*<0.05, ****P*<0.001.
Abbreviation: ns, no significance.

https://doi.org/10.2147/JIR.S518829

On the fourth day post-induction, a statistical difference emerged between the CON group and both the MIA and FNA groups, indicating joint discomfort as evidenced by asymmetric weight distribution. MIA treatment resulted in a significant reduction in weight bearing on the ipsilateral limb from day 4 until the end of the observation period (Figure 1D). All animals initially exhibited similar responses in the mechanical allodynia test (paw withdrawal threshold), with no statistical differences among groups. However, by day 4 after MIA induction, a significant reduction in paw withdrawal threshold was observed in the MIA and FNA groups compared to the CON group. This decrease in nociceptive threshold persisted throughout the experiment, lasting until day 29 following MIA injection (Figure 1E).

In comparison to the MIA group, the FNA treatment groups demonstrated gradual improvement. Following fire needling acupuncture treatment, pain avoidance behaviors were observed to reverse gradually. At all assessed time points post-treatment, rats in the FNA group exhibited less severe weight bearing deficits compared to those in the MIA group (Figure 1D). Additionally, the FNA group showed a significant reduction in bilateral weight bearing differences compared to the MIA group, with statistical significance. All animals responded similarly in the paw withdrawal threshold assessments (Figure 1E). Notably, the mechanical withdrawal thresholds of the FNA groups significantly increased following three sessions of fire needling acupuncture treatment, with these differences reaching statistical significance.

Reduction of Inflammation and Modulation of Macrophage Polarization in Synovial Tissues by Fire Needling Acupuncture in KOA Rats

HE and Saf-O staining were conducted to further investigate the effects of fire needling acupuncture on synovial inflammation (Figure 4A). The cellularity and structural changes of the synovial tissues were assessed by evaluating hypercellularity of the synovial membrane and alterations in tissue structure. Rats that received saline injections exhibited an intact synovial surface, a single layer of lining cells, normal synovial stroma cells, and no signs of inflammatory infiltration. In contrast, MIA injection resulted in a significant increase in the number of synovial lining cells and stromal cells, accompanied by infiltration of numerous lymphocytes and plasma cells. In the FNA group, fewer lining cells, stromal cells, and infiltrating lymphocytes or plasma cells were observed compared to the MIA group. These histological findings were semi-quantitatively evaluated using a scoring system as previously described,[26] with results presented in Figure 4E. After 29 days of intra-articular injection, the synovitis score in the MIA group was significantly higher than in the CON group. Following fire needling acupuncture treatment, the synovitis score decreased.

Additionally, we employed immunofluorescence staining to examine the inflammatory-modulating effects of fire needling acupuncture on the synovial tissue of KOA rats. Our observations revealed that the M0 macrophage surface marker F4/80 and the M1-type macrophage marker iNOS were significantly elevated in the MIA group compared to the CON group, while the M2-type macrophage marker Arg-1 was decreased (Figure 4B–D). In the FNA group, F4/80 and iNOS levels were reduced, and Arg-1 levels were increased compared to the MIA group. The quantitative results of these markers are shown in Figure 4F–H. These findings confirm that fire needling acupuncture effectively alleviates the microenvironment of KOA by reducing the expression of inflammatory factors and modulating macrophage polarization in the synovium. This intervention appears to retard the progression of KOA, aligning with the therapeutic objectives of OA treatment.

Modification of Subchondral Bone Degradation in KOA Rats Through Fire Needling Acupuncture Treatment

Subsequent observations of subchondral bone changes were conducted. In our study, no OA-like alterations were noted in the subchondral bone microstructure of normal control knee joints (Figure 5B). However, micro-CT imaging revealed a reduction and narrowing of the trabecular bone structure following MIA injection, accompanied by significant joint damage, subchondral bone plate fractures, and the formation of subchondral bone cysts. Throughout the 4-week study period, all rats injected with MIA exhibited pathological changes in the subchondral bone of the knee joints, characterized by extensive replacement of local subchondral bone marrow areas with loosely arranged spindle cells, indicative of fibrotic bone marrow. Morphological evaluations of the MIA-injected knees demonstrated subchondral ossification

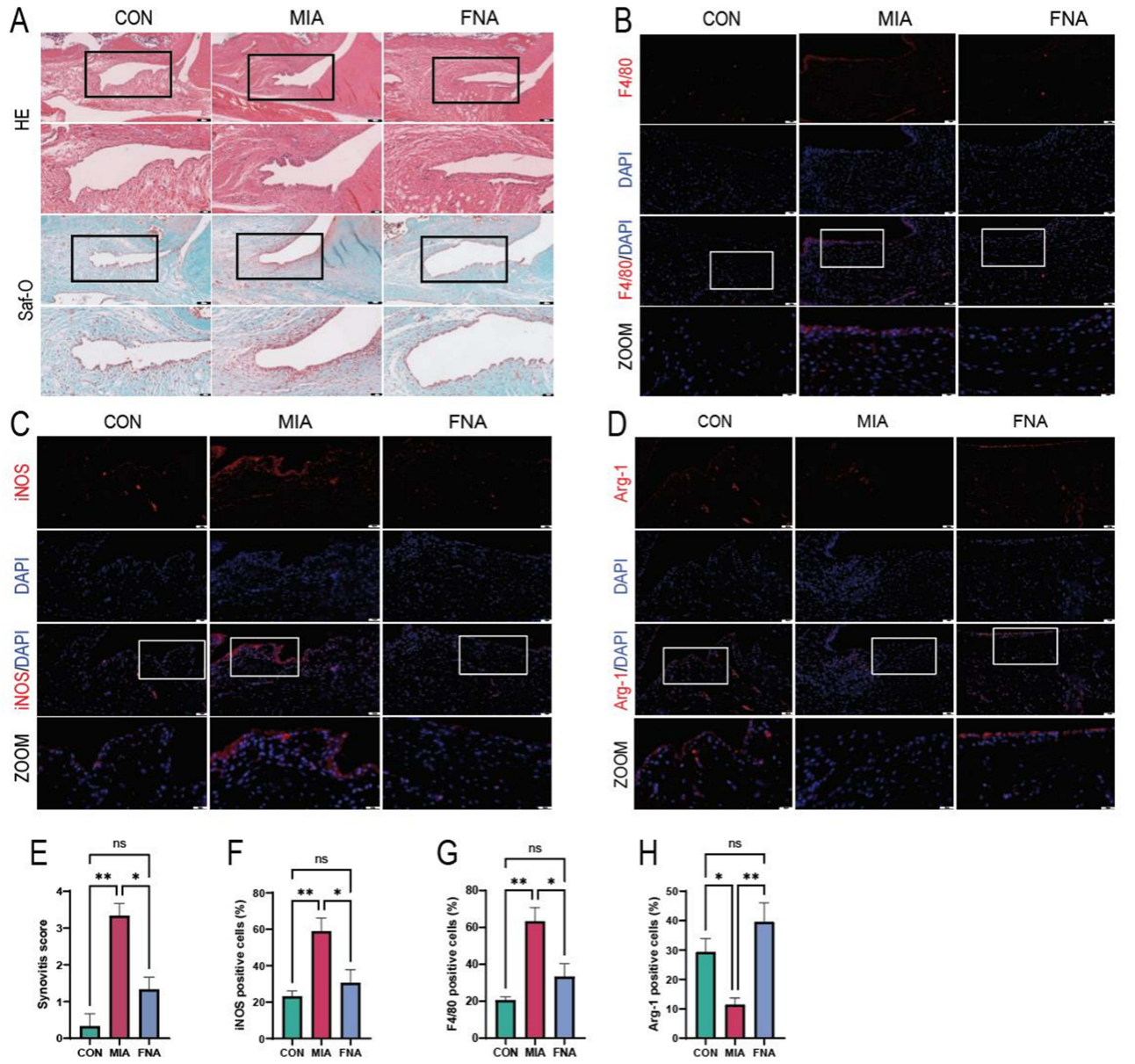

Figure 4 (**A**) Images of HE staining and Saf-O staining of the synovium of rat knee joint. Scale bars = 100μm or 40μm. (**B–D**) Images of Immunofluorescence staining of F4/80, iNOS and Arg-1 of the synovium of rat knee joint. Scale bars = 40μm or 20μm. (**E**) Quantification of synovial inflammation scores. (**F–H**) Quantification of the number of positive cells of F4/80, iNOS and Arg-1. Data are expressed as the mean ± SEM, n = 3 for each group. **P*<0.05, ***P*<0.01.
Abbreviation: ns, no significance.

(osteophyte) and focal fractures of the tibial subchondral plate, which were histologically confirmed (Figure 5A and B). Histological examinations revealed that the subchondral bone of the MIA-injected knee was compromised, with cavities identified as cysts (Figure 5A). Additionally, a significant presence of osteoclasts was observed surrounding the subchondral bone cysts (Figure 5C). In comparison to the MIA group, the subchondral bone injury following fire needling acupuncture treatment was less pronounced. The subchondral bone plate appeared more intact, the arrangement of the bone trabeculae was more orderly, the subchondral bone cysts were smaller (Figure 5A and B), and the number of osteoclasts was reduced (Figure 5C and D). There was no statistically significant difference in TRAP levels between the CON and FNA groups; however, both groups exhibited a statistically significant difference when compared to the MIA group (Figure 5D). These results demonstrated that fire needling acupuncture therapy reduced subchondral bone structural damage and delayed the progression of KOA rats.

https://doi.org/10.2147/JIR.S518829

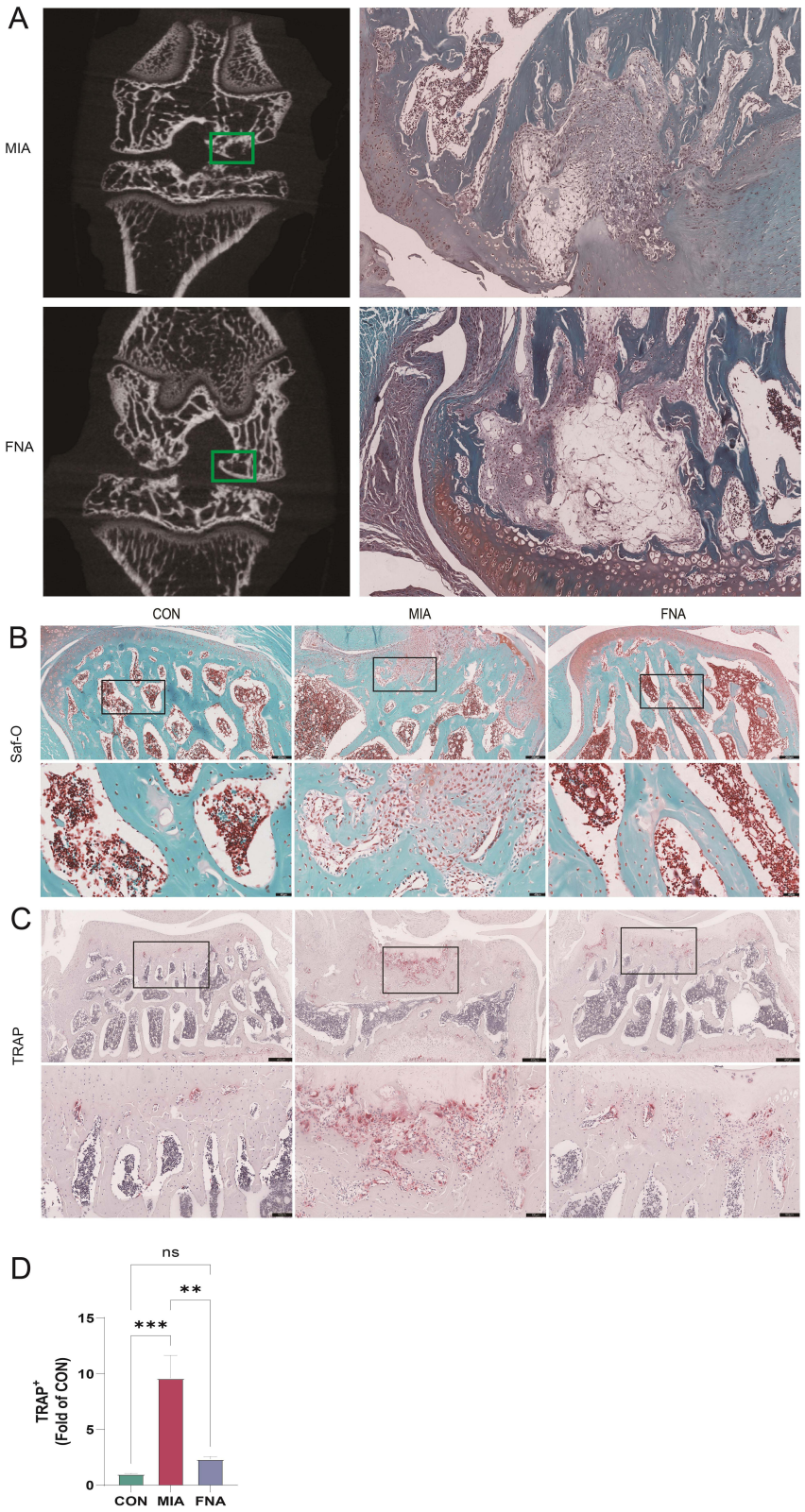

Figure 5 (**A**) Micro-CT images and Saf-O staining images. The green rectangles represent subchondral bone cysts. (**B**) Saf-O staining images of subchondral bone of KOA. Scale bars = 200μm or 40μm. (**C**) TRAP staining images of subchondral bone of KOA. Scale bars = 400μm or 100μm. (**D**) Quantification of $TRAP^+$. Data are expressed as the mean ± SEM, n = 3 for each group. $^{**}P<0.01$, $^{***}P<0.001$.
Abbreviation: ns, no significance.

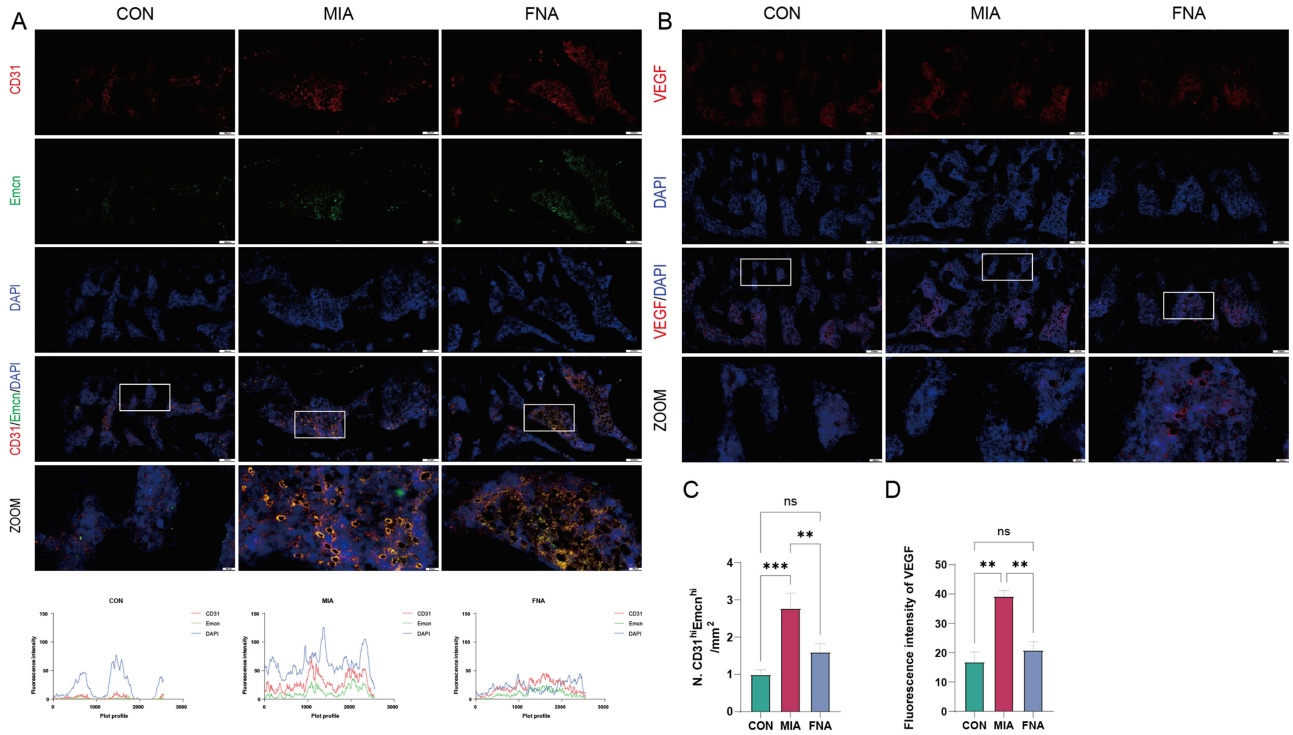

Figure 6 (**A**) Images of Immunofluorescence staining and fluorescence intensity of CD31/Emcn of rat knee joints. Scale bars = 200μm or 40μm. (**A** and **B**) Images of Immunofluorescence staining of VEGF of rat knee joints. Scale bars = 200μm or 40μm. (**C**) Quantification of $CD31^{hi}/Emcn^{hi}$. (**D**) Quantification of VEGF. Data are expressed as the mean ± SEM, n = 3 for each group. ***P*<0.01, ****P*<0.001.
Abbreviation: ns, no significance.

Effects of Subchondral Bone Angiogenesis Markers by Fire Needling Acupuncture Treatment in KOA Rats

In the study of KOA, the microenvironment of subchondral bone and its angiogenic characteristics have garnered significant attention. This study evaluated the changes in the expression of CD31, endomucin (Emcn), and vascular endothelial growth factor (VEGF) in the subchondral bone of a MIA-induced KOA model, as well as the effects of fire needling acupuncture therapy. Following joint injection of MIA, the expression of CD31/Emcn and VEGF in the subchondral bone was significantly increased (Figure 6A–D), reflecting enhanced angiogenic activity under the inflammatory conditions induced by MIA, which may contribute to cartilage damage and disease progression. Further investigation revealed that fire needling therapy significantly reduced the expression levels of CD31/Emcn and VEGF in the subchondral bone of KOA models. These findings suggest that fire needling acupuncture therapy may improve the microenvironment of subchondral bone by inhibiting abnormal angiogenesis and inflammatory responses, thereby providing protective effects against the pathological progression of KOA.

Discussion

OA is characterized by the progressive destruction of cartilage, loss of extracellular matrix proteins, and damage to articular cartilage due to various factors.[28] Recent studies have emphasized the critical roles of the synovium and subchondral bone in the pathogenesis and progression of OA.[3,29] This study investigates the effects of fire needling on MIA-induced KOA in rats. There is substantial evidence indicating significant improvements in weight distribution and mechanical withdrawal thresholds, alongside a reduction in synovial inflammation and enhanced cartilage integrity. Notably, fire needling acupuncture treatment downregulated the expression of M0 macrophage marker F4/80 and M1 macrophage marker iNOS, while upregulating the expression of M2 macrophage marker Arg-1. Additionally, the subchondral bone angiogenesis markers CD31/Emcn and VEGF were found to be reduced.

https://doi.org/10.2147/JIR.S518829

We observed that, compared to the CON group, rats with MIA-induced KOA exhibited OA symptoms, including more pronounced weight-bearing imbalance, lower mechanical withdrawal thresholds, severe loss of proteoglycans, more significant cartilage damage, increased synovial inflammation, and abnormal changes in subchondral bone. The structure of the articular cartilage was severely compromised. Cracks and indentations appeared on the cartilage surface, and there was a significant reduction in cartilage thickness (Figure 2A–C). This degeneration impaired the cartilage's cushioning function, increasing joint friction and resulting in pain and functional impairment. Additionally, MIA injection caused hypertrophy and death of chondrocytes, with significant elevations in cartilage damage biomarkers, including MMP9 and MMP13, and a marked decrease in COL2 levels (Figure 3). As the primary component of articular cartilage, the expression of COL2 was significantly reduced after MIA-induced, indicating compromised structural stability.[30,31] Concurrently, the expression of MMP9 and MMP13 was significantly enhanced, both of which are associated with the degradation of cartilage matrix.[32] The increase in MMP9 promotes collagen breakdown, while MMP13 specifically targets the degradation of COL2, collectively accelerating the degenerative process of cartilage.[33,34] On the one hand, the synovium displayed a marked inflammatory response characterized by thickening and cellular infiltration, particularly with the accumulation of macrophages, lymphocytes, and plasma cells (Figure 4A). The expression of the M0 macrophage marker (F4/80) and M1 type (iNOS) was elevated, while M2 type (Arg-1) expression was reduced (Figures 4B–D). These findings are consistent with previously reported changes in macrophages in KOA models,[35–37] suggesting that macrophage polarization is one of the extremely important key aspects of the pathological mechanism of OA.[38] This inflammatory state leads to increased secretion of inflammatory factors from the synovium, further exacerbating joint inflammation.[39] On the other hand, the structure of the subchondral bone was also affected. Due to cartilage degeneration, there was a significant decrease in bone density in the subchondral region, with noticeable thinning of the trabecular framework. Following MIA injection, microfractures and bone cysts were observed in the subchondral bone (Figure 5A), consistent with findings by Januz et al,[40] further impacting joint stability and function.

In KOA, the expression of TRAP is increased (Figure 5C and D), indicating enhanced osteoclast activity, which may contribute to the interaction between bone resorption and cartilage damage, leading to osteoporosis and the destruction of trabecular bone.[41,42] In the MIA-induced KOA model, it was observed that the expression of angiogenesis markers CD31/Emcn and VEGF in the subchondral bone was significantly elevated.[43,44] This phenomenon suggests that angiogenic activity in the subchondral bone is enhanced in pathological states, potentially correlating with the progression of arthritis. CD31 and Emcn are characteristic markers of vascular endothelial cells, reflecting the formation of new blood vessels, and their co-expression aids in identifying h-type vessels, while VEGF is a key factor promoting angiogenesis.[45] The increase in these markers may lead to changes in the microenvironment of the subchondral bone, subsequently affecting the nutritional supply and repair capacity of the cartilage. By promoting angiogenesis, this process may partially alleviate the ischemic state of the cartilage; however, it may also lead to abnormal vessel formation, which could further exacerbate the inflammatory response and cartilage damage.[46] Furthermore, the mechanisms underlying the macrophage-angiogenesis crosstalk remain unclear and warrant further exploration in future studies.

The treatment of KOA presents challenges. Non-pharmacological therapies have relatively few side effects, are suitable for long-term management and offer a safe, effective option. Acupuncture has shown promising results in treating KOA,[47] and fire needling acupuncture therapy, as a traditional method, has also been recommended in this context.[48] Fire needling acupuncture therapy may positively impact subchondral bone by promoting local blood circulation and alleviating muscle tension.[49] This study employs clinical experience and literature analysis to utilize fire needle acupuncture at the surrounding points of the knee joint, specifically ST34, ST35, ST36, SP10, and EX-LE5, for treatment.[47,50] Behavioral testing indicated that fire needling acupuncture reduced weight-bearing differences and increased mechanical withdrawal thresholds. Post-treatment observations indicate that fire needling acupuncture therapy modulates macrophage polarization in the synovium of KOA by reducing the expression of M0 macrophage marker F4/80 and M1 macrophage marker (iNOS), while enhancing the expression of M2 macrophage marker (Arg-1), thereby alleviating synovial inflammation. Additionally, there was a decrease in cartilage structural damage, an increase in COL2 expression, and a reduction in MMP9 and MMP13 expression, leading to a more intact structure of subchondral bone, along with decreased expression of TRAP, VEGF, and CD31/Emcn. In summary, preliminary research has demonstrated the potential of fire needling acupuncture therapy to alleviate pain, reduce cartilage damage, regulate macrophage polarization, and improve the microenvironment of subchondral bone (Figure 7). Future research should further explore the mechanisms of fire needling treatment, particularly the interaction between macrophage polarization and angiogenesis.

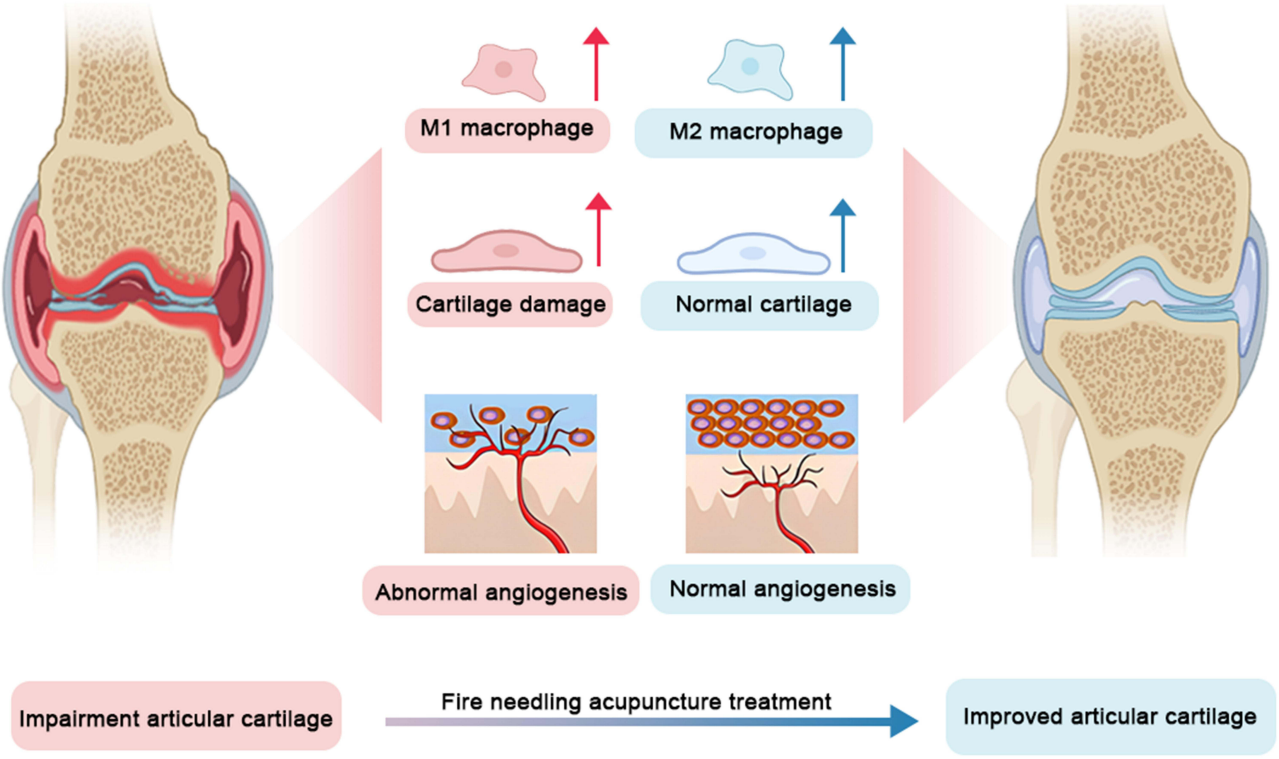

Figure 7 Schematic diagram illustrating how fire needling acupuncture regulates macrophage polarization, reduces cartilage damage, and inhibits abnormal angiogenesis in the subchondral bone.

This study has several limitations. First of all, the use of a single model without multi-model validation may restrict the conclusions drawn. In addition, the absence of observations across different time windows may hinder the ability to capture the full scope of angiogenesis and inflammatory responses, preventing a comprehensive understanding of the biological characteristics of subchondral bone and its relationship with cartilage degeneration. Furthermore, this study utilized male Sprague-Dawley rats, and future research is needed to explore sex-specific effects to enhance the overall impact and applicability of our findings.

Conclusion

In conclusion, fire needling acupuncture effectively reduces pain behaviors in KOA rats and ameliorates synovial membrane injury, cartilage damage, and subchondral bone degeneration. The therapeutic mechanism appears to involve synovial macrophage polarization and subchondral bone angiogenesis, contributing to the improvement of articular cartilage impairment. Future research should further investigate the interaction between macrophage polarization and angiogenesis.

Data Sharing Statement

Data sets generated and analyzed during the current study are available from the corresponding authors upon reasonable request.

Funding

This work was supported by the following funding sources: the National Natural Science Foundation of China (82274642, 82474631, 82074547 and 82205246); Beijing Hospital Management Center “peak” talent training plan team (DFL20241001); the fifth batch of national TCM clinical outstanding talents project.

Disclosure

The authors declare no potential conflicts of interest concerning this article's research, authorship, and/or publication.

References

1. Sharma L. Osteoarthritis of the knee. *New Engl J Med*. 2021;384(1):51–59. doi:10.1056/NEJMcp1903768
2. Alice C, Inès K, Nadine S, Sylvain M, Jérémie S. Osteoarthritis year in review 2024: epidemiology and therapy. *Osteoarthr Cartilage*. 2024;32(11):1397–1404.
3. Jiang Y. Osteoarthritis year in review 2021: biology. *Osteoarthr Cartilage*. 2022;30(2):207–215. doi:10.1016/j.joca.2021.11.009
4. Collaborators GO. Global, regional, and national burden of osteoarthritis, 1990–2020 and projections to 2050: a systematic analysis for the Global Burden of Disease Study 2021. *Lancet Rheumatol*. 2023;5(9):e508–e522. doi:10.1016/S2665-9913(23)00163-7
5. Bannuru RR, Osani MC, Vaysbrot EE, et al. OARSI guidelines for the non-surgical management of knee, Hip, and polyarticular osteoarthritis. *Osteoarthr Cartilage*. 2019;27(11):1578–1589. doi:10.1016/j.joca.2019.06.011
6. Moore N, Salvo F, Duong M, Gulmez SE. Does paracetamol still have a future in osteoarthritis? *Lancet*. 2016;387(10033):2065–2066. doi:10.1016/S0140-6736(15)01170-8
7. Pirri C, Sorbino A, Manocchio N, et al. Chondrotoxicity of Intra-Articular Injection Treatment: a Scoping Review. *Int J Mol Sci*. 2024;25(13):7010. doi:10.3390/ijms25137010
8. Moseng T, Vliet VT, Battista S, et al. EULAR recommendations for the non-pharmacological core management of hip and knee osteoarthritis: 2023 update. *Ann Rheum Dis*. 2024;83(6):730–740.
9. Du X, Wen X, Liu D, et al. Preliminary study on the therapeutic effect and effect mechanism of fire -needling. *J Clin Acupunct Moxibustion*. 2018;34(9):1–4.
10. Yu P, Li Z, Liu L, Wang Y, Xu X, Li B. Discussion on the development of the effect of fire needling based on the changes of diseases types treated with fire needling in past dynasties. *J Traditional Chin Med*. 2020;61(16):1410–1413.
11. Xin S, Liu J, Yang Z, Li C. Comparative effectiveness of moxibustion and acupuncture for the management of osteoarthritis knee: a systematic review and meta-analysis. *Heliyon*. 2023;9(7):e17805. doi:10.1016/j.heliyon.2023.e17805
12. Liu W, Fan Y, Wu Y, et al. Efficacy of acupuncture-related therapy in the treatment of knee osteoarthritis: a network meta-analysis of randomized controlled trials. *J Pain Res*. 2021;14:2209–2228. doi:10.2147/JPR.S315956
13. Wei J, Liu L, Li Z, et al. Fire needling acupuncture suppresses cartilage damage by mediating macrophage polarization in mice with knee osteoarthritis. *J Pain Res*. 2022;15:1071–1082. doi:10.2147/JPR.S360555
14. Li Z, Wang X, Sun J, et al. Effect of fire-needle intervention on joint function, cartilage impairment and inflammatory response in knee osteoarthritis rats. *Zhen Ci Yan Jiu*. 2020;45(3):220–226. doi:10.13702/j.1000-0607.190963
15. Li G, Yin J, Gao J, et al. Subchondral bone in osteoarthritis: insight into risk factors and microstructural changes. *Arthritis Res Ther*. 2013;15(6):223. doi:10.1186/ar4405
16. Hu W, Chen Y, Dou C, Dong S. Microenvironment in subchondral bone: predominant regulator for the treatment of osteoarthritis. *Ann Rheum Dis*. 2021;80(4):413–422. doi:10.1136/annrheumdis-2020-218089
17. Dieppe PA, Lohmander LS. Pathogenesis and management of pain in osteoarthritis. *Lancet*. 2005;365(9463):965–973. doi:10.1016/S0140-6736(05)71086-2
18. Lin C, Liu L, Zeng C, et al. Activation of mTORC1 in subchondral bone preosteoblasts promotes osteoarthritis by stimulating bone sclerosis and secretion of CXCL12. *Bone Res*. 2019;7:5. doi:10.1038/s41413-018-0041-8
19. Atukorala I, Kwoh CK, Guermazi A, et al. Synovitis in knee osteoarthritis: a precursor of disease? *Ann Rheum Dis*. 2016;75(2):390–395. doi:10.1136/annrheumdis-2014-205894
20. Zhu X, Lee CW, Xu H, et al. Phenotypic alteration of macrophages during osteoarthritis: a systematic review. *Arthritis Res Ther*. 2021;23(1):110. doi:10.1186/s13075-021-02457-3
21. Zhu S, Zhu J, Zhen G, et al. Subchondral bone osteoclasts induce sensory innervation and osteoarthritis pain. *J Clin Invest*. 2019;129(3):1076–1093. doi:10.1172/JCI121561
22. La Porta C, Bura SA, Aracil-Fernandez A, Manzanares J, Maldonado R. Role of CB1 and CB2 cannabinoid receptors in the development of joint pain induced by monosodium iodoacetate. *Pain*. 2013;154(1):160–174. doi:10.1016/j.pain.2012.10.009
23. Moxibustion, China Institute of Acupuncture. Name and location of commonly used acupoints in laboratory animals - Part 2: rats. *Acupuncture Res*. 2021;46(4):351–352.
24. Deshmukh V, O'Green AL, Bossard C, et al. Modulation of the Wnt pathway through inhibition of CLK2 and DYRK1A by lorecivivint as a novel, potentially disease-modifying approach for knee osteoarthritis treatment. *Osteoarthr Cartilage*. 2019;27(9):1347–1360. doi:10.1016/j.joca.2019.05.006
25. Chaplan SR, Bach FW, Pogrel JW, Chung JM, Yaksh TL. Quantitative assessment of tactile allodynia in the rat paw. *J Neurosci Meth*. 1994;53(1):55–63. doi:10.1016/0165-0270(94)90144-9
26. Krenn V, Morawietz L, Burmester G, et al. Synovitis score: discrimination between chronic low-grade and high-grade synovitis. *Histopathology*. 2006;49(4):358–364. doi:10.1111/j.1365-2559.2006.02508.x
27. Pritzker KP, Gay S, Jimenez SA, et al. Osteoarthritis cartilage histopathology: grading and staging. *Osteoarthr Cartilage*. 2006;14(1):13–29. doi:10.1016/j.joca.2005.07.014
28. Fujii Y, Liu L, Yagasaki L, Inotsume M, Chiba T, Asahara H. Cartilage Homeostasis and Osteoarthritis. *Int J Mol Sci*. 2022;23(11):6316. doi:10.3390/ijms23116316
29. Roelofs AJ, De Bari C. Osteoarthritis year in review 2023: biology. *Osteoarthr Cartilage*. 2023;32(2):148–158.
30. Tian Y, Gou J, Zhang H, et al. The anti-inflammatory effects of 15-HETE on osteoarthritis during treadmill exercise. *Life Sci*. 2021;273:119260. doi:10.1016/j.lfs.2021.119260
31. Chen Z, Zhou L, Ge Y, et al. Fuzi decoction ameliorates pain and cartilage degeneration of osteoarthritic rats through PI3K-Akt signaling pathway and its clinical retrospective evidence. *Phytomedicine*. 2022;100:154071. doi:10.1016/j.phymed.2022.154071

32. Chun JM, Lee AY, Moon BC, Choi G, Kim JS. Effects of Dipsacus asperoides and Phlomis umbrosa extracts in a rat model of osteoarthritis. *Plants-Basel*. 2021;10(10):2030.
33. Chen Z, Ge Y, Zhou L, et al. Pain relief and cartilage repair by Nanofat against osteoarthritis: preclinical and clinical evidence. *Stem Cell Res Ther*. 2021;12(1):477. doi:10.1186/s13287-021-02538-9
34. Kwon SB, Chinta G, Kundimi S, et al. A blend of Tamarindus Indica and Curcuma Longa extracts Alleviates Monosodium Iodoacetate (MIA)-induced osteoarthritic pain and joint inflammation in rats. *J Am Nutr Assoc*. 2024;43(1):48–58. doi:10.1080/27697061.2023.2209880
35. Zhang H, Lin C, Zeng C, et al. Synovial macrophage M1 polarisation exacerbates experimental osteoarthritis partially through R-spondin-2. *Ann Rheum Dis*. 2018;77(10):1524–1534. doi:10.1136/annrheumdis-2018-213450
36. Pang L, Jin H, Lu Z, et al. Treatment with mesenchymal stem cell-derived nanovesicle-containing gelatin methacryloyl hydrogels alleviates osteoarthritis by modulating chondrogenesis and macrophage polarization. *Adv Healthc Mater*. 2023;12(17):e2300315. doi:10.1002/adhm.202300315
37. Zhang Y, Ji Q. Macrophage polarization in osteoarthritis progression: a promising therapeutic target. *Front Cell Dev Biol*. 2023;11:1269724. doi:10.3389/fcell.2023.1269724
38. Zhang H, Cai D, Bai X. Macrophages regulate the progression of osteoarthritis. *Osteoarthr Cartilage*. 2020;28(5):555–561. doi:10.1016/j.joca.2020.01.007
39. Mathiessen A, Conaghan PG. Synovitis in osteoarthritis: current understanding with therapeutic implications. *Arthritis Res Ther*. 2017;19(1):18. doi:10.1186/s13075-017-1229-9
40. Janusz MJ, Hookfin EB, Heitmeyer SA, et al. Moderation of iodoacetate-induced experimental osteoarthritis in rats by matrix metalloproteinase inhibitors. *Osteoarthr Cartilage*. 2001;9(8):751–760. doi:10.1053/joca.2001.0472
41. Zheng X, Qiu J, Gao N, et al. Paroxetine attenuates chondrocyte pyroptosis and inhibits osteoclast formation by inhibiting NF-kappaB pathway activation to delay osteoarthritis progression. *Drug Des Devel Ther*. 2023;17:2383–2399. doi:10.2147/DDDT.S417598
42. He Z, Nie P, Lu J, et al. Less mechanical loading attenuates osteoarthritis by reducing cartilage degeneration, subchondral bone remodelling, secondary inflammation, and activation of NLRP3 inflammasome. *Bone Joint Res*. 2020;9(10):731–741. doi:10.1302/2046-3758.910.BJR-2019-0368.R2
43. Li HZ, Han D, Ao RF, et al. Tanshinone IIA attenuates osteoarthritis via inhibiting aberrant angiogenesis in subchondral bone. *Arch Biochem Biophys*. 2024;753:109904. doi:10.1016/j.abb.2024.109904
44. Cui Z, Crane J, Xie H, et al. Halofuginone attenuates osteoarthritis by inhibition of TGF-beta activity and H-type vessel formation in subchondral bone. *Ann Rheum Dis*. 2016;75(9):1714–1721. doi:10.1136/annrheumdis-2015-207923
45. Nagao M, Hamilton JL, Kc R, et al. Vascular endothelial growth factor in cartilage development and osteoarthritis. *Sci Rep*. 2017;7(1):13027. doi:10.1038/s41598-017-13417-w
46. Lu J, Zhang H, Cai D, et al. Positive-feedback regulation of subchondral H-type vessel formation by chondrocyte promotes osteoarthritis development in mice. *J Bone Miner Res*. 2018;33(5):909–920. doi:10.1002/jbmr.3388
47. Tu JF, Yang JW, Shi GX, et al. Efficacy of intensive acupuncture versus Sham acupuncture in knee osteoarthritis: a randomized controlled trial. *Arthritis Rheumatol*. 2021;73(3):448–458. doi:10.1002/art.41584
48. Wang H. Expert consensus on the treatment of knee osteoarthritis (Knee Arthralgia) by integrated Traditional Chinese and Western Medicine. *World Chin Med*. 2023;18(17):2407–2412.
49. Zhao L, Liu L, Wang Y, et al. Preliminary study on the "breaking" and "building" effects of fire acupuncture therapy and its clinical application. *J Traditional Chin Med*. 2019;60(14):1255–1257.
50. Shim JW, Jung JY, Kim SS. Effects of electroacupuncture for knee osteoarthritis: a systematic review and meta-analysis. *Evid-Based Complementary Altern Med*. 2016;2016:3485875. doi:10.1155/2016/3485875